APPLICATION OF ONSET THEORY TO ONSET OF TRANSVERSE CRACKING IN FABRIC COMPOSITES

S. H. Lim[1,2], G. Pearce[1]*, D. Kelly[1], B. G. Prusty[1] and A. Crosky[3]

[1] UNSW Mechanical and Manufacturing Engineering, UNSW Australia, Sydney, Australia
[2] School of Engineering, The University of Waikato, Hamilton, New Zealand
[3] UNSW Materials Science and Engineering, UNSW Australia, Sydney, Australia
*Email: g.pearce@unsw.edu.au

Keywords: Onset Theory, SIFT, Fibre Reinforced Polymers, Micromechanical Modelling

ABSTRACT

A paper presented at ICCM-19 included a methodology for application of Onset Theory to the prediction of microcracking in the transverse plies of orthogonal [0/90] fabric laminates. This paper applies the methodology to predict damage locations and laminate strains for failure of plain weave fabric specimens manufactured from two material systems – HTS40/RTM6 and T300/CYCOM970. The laminate strains are first dehomogenised to define local strains in the tow architecture of the fabric. This is achieved using meso-mechanical unit cell analysis in which the resin and tows are modelled as continua. For a selection of predefined critical locations in the tow bundles, the strains are further dehomogenised using an identical procedure as the one defined for the uni-directional specimens in the previous applications. The influence of matrix plasticity and temperature dependent mechanical and thermal properties of the RTM6 resin are applied in the dehomogenisation procedure. The Onset theory predictions for damage locations were compared to those obtained from microscopic surveys of partially failed plain weave fabric specimens.

1 INTRODUCTION

Onset Theory (previously known as Strain Invariant Failure Theory SIFT) was first proposed by Gosse and Christensen [1] and applied to fibre and resin failure in composites manufactured from uni-directional plies. In their work results from finite element analysis of laminates manufactured from unitape are dehomogenised to define strains in the resin and fibre phases of the composite. The dehomogenisation can be achieved using enhancement factors derived from a micromechanical analysis of a unit cell (Pipes and Gosse [2]) or obtained from a local three-dimensional finite element model of resin and fibre (Tran et al [3, 4]). The local strains are used to define two invariants which represent the dilatational and distortional deformation of the resin.

The Onset Theory of failure is based on two fundamental assertions. The first assertion is that prediction of failure of constrained viscoelastic homogeneous materials should be based on strain. The second assertion is that the onset of irreversible behaviour in glassy polymer resins can occur only via excessive dilatation (volume change) or excessive distortion (shape change). Only two intrinsic material properties are therefore required to characterise these failures, based on the first strain invariant (dilatation) and the second deviatoric (distortional) strain invariant. It will be noted in this work that the prediction of failure will only coincide with the appearance of microcracks for glassy (brittle) materials. For ductile materials the growth of cracks that can be observed may only follow a further increment to the strain.

In the approach defined by Pipes and Gosse [2], critical values for the strain invariants are defined for the dilatational and distortional invariants for the resin using 90 degree and 10 degree unidirectional off-axis test specimens respectively. However, validation of the theory has been provided by Christensen [5] and Sul et al. [6-8] by reproducing the critical values of the strain invariants using molecular dynamics simulations completely independently of the experimental approach. In this paper Onset Theory will be applied to predict damage locations and laminate strains for failure of plain weave fabric specimens manufactured from two material systems – HTS40/RTM6 and T300/CYCOM970. The molecular dynamics approach is implemented to define the critical

invariants for the RTM6 resin. The research team were unable to source uni-directional specimens of industrial quality for the HTS40/RTM6 material system.

2 REVIEW OF ONSET THEORY

2.1 Strain Invariants

Onset Theory is a failure theory developed for glassy polymers constrained by fibres in structural composites. The theory simply posits that the constrained polymer will fail when subjected to excessive deformation; either through excessive volume change (dilatation) or excessive shape change (distortion). This fundamental property of polymer materials is founded in thermodynamic theory and has been confirmed by atomistic simulation of polymers [6-8]. To quantify dilatation and distortion, strain invariants are used, related to the fundamental invariants of the strain tensor. The dilatational invariant is equal to the first strain invariant, J_1, and is shown in Equation 1. The distortional invariant is equal to the square root of the second deviatoric strain invariant, $J_2^{'}$, and is shown in Equation 2.

$$\varepsilon_{dil} = \varepsilon_1 + \varepsilon_2 + \varepsilon_3 = \varepsilon_x + \varepsilon_y + \varepsilon_z \tag{1}$$

$$\begin{aligned} \varepsilon_{dis} &= \sqrt{\frac{1}{6}\left[(\varepsilon_1 - \varepsilon_2)^2 + (\varepsilon_2 - \varepsilon_3)^2 + (\varepsilon_3 - \varepsilon_1)^2\right]} \\ &= \sqrt{\frac{1}{6}\left[(\varepsilon_x - \varepsilon_y)^2 + (\varepsilon_y - \varepsilon_z)^2 + (\varepsilon_z - \varepsilon_x)^2\right] + \frac{1}{4}\left[{\gamma_{xy}}^2 + {\gamma_{yz}}^2 + {\gamma_{xz}}^2\right]} \end{aligned} \tag{2}$$

where:

ε_{dil} = Dilatational strain invariant

ε_{dis} = Distortional strain invariant

$\varepsilon_{1,2,3}$ = Principal elastic strains

$\varepsilon_{x,y,z}, \gamma_{xy,yz,xz}$ = Engineering elastic strain tensor in Cartesian coordinates

Irreversible behaviour is predicted to occur when either the dilatational or distortional strain invariant at any location in the resin exceeds the corresponding critical value, $\varepsilon_{dil,crit}$ or $\varepsilon_{dis,crit}$. The two critical strain invariants are considered intrinsic material properties.

2.2 Effect of Temperature

Onset theory explicitly accounts for the thermal residual strains present in constrained resin by only evaluating strain invariants using *elastic* strains; those which are compatible with the stress tensor through Hooke's Law, as shown in Equation 3.

$$\{\boldsymbol{\varepsilon}\} = [\mathbf{S}]\{\boldsymbol{\sigma}\} \tag{3}$$

For a fully constrained 3D element of resin subjected to a positive temperature increment, ΔT, the principal elastic strains are given by Equation 4.

$$\varepsilon_{1,2,3} = -\alpha \Delta T \tag{4}$$

where α is the linear coefficient of thermal expansion (CTE) for the resin. Therefore, strain due to the thermal shrinkage of free resin does not contribute to failure. On the other hand, shrinkage of constrained resin, such as that constrained by fibres, leads to a non-zero elastic strain tensor, which can contribute to failure. All strain tensor terms shown in this paper are taken from the elastic strain tensor.

2.3 Dehomogenisation

An important feature of the onset theory is the dehomogenisation of the composite structure. This process allows determination of the components of the strain tensor field within the matrix phase and

fibre phase [2] and enables damage prediction within a complex structural domain, such as the random distribution of fibres and resin shown in Figure 1(a). With this process, the thermal residual effect due to the thermal contraction mismatch of fibre and resin is also taken into account. Two Representative Volume Elements (RVEs) are used to account for the distribution of fibres and resin within the composite, shown in Figure 1(b). The justification and validation of this approach is given in [9].

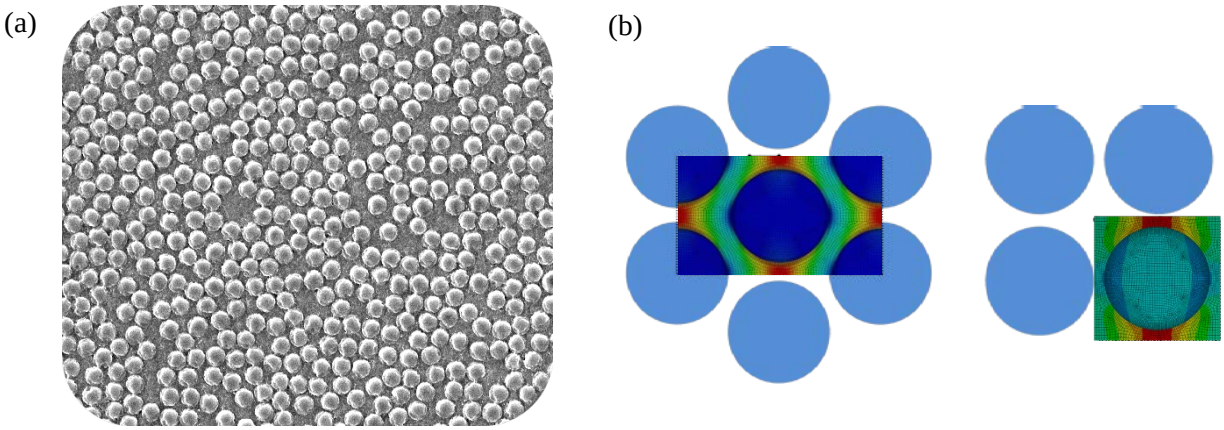

Figure 1: (a) Realistic distribution of fibres and resin within a composite and (b) Idealised Representative Volume Elements (RVEs) with the same volume fraction (Vf).

A series of critical points, *k*, are used as sampling points within the RVE at which the critical invariants are evaluated. At each point, *k*, a matrix of *enhancement factors*, $\mathbf{M}^k$, is generated which relates the strain tensor at the sampling point, $\boldsymbol{\varepsilon}^k$, to the continuum strain tensor, $\mathbf{E}$, obtained from a continuum analysis of the ply. A thermal strain vector, $\mathbf{A}^k$, also defined at every point, accounts for the residual strain present in an unconstrained ply ($\mathbf{E}=\mathbf{0}$) due to the local mismatch in thermal expansion between the fibre and resin, for a unit temperature change. Algorithmically, the dehomogenisation process can be expressed for laminates made from unidirectional plies as follows:

1. Analyse an unconstrained continuum model with imposed thermal condition, $\Delta T = T - T_{cure}$, to define the *thermomechanical* elastic strain, $\mathbf{E}^T$, in the plies due to the cure process.
2. Analyse a continuum model with mechanical load to define the *mechanical* elastic strain, $\mathbf{E}^M$, in the plies. (Note that in many FE codes, steps 1 and 2 can be conducted, in series, during the same solution run. In these cases, the calculated elastic strain at the end of step 2 already includes the thermal contribution. There are challenges involved with this technique: it must be ensured that the boundary conditions during the thermomechanical step do not impose any global constraint on the model; also, the mechanical loads/displacements for step 2 must be applied relative to the deformed model state at the end of step 1.)
3. As a post-processing operation, superimpose the mechanical and thermomechanical elastic strain. Apply the strain enhancement factors and add the cure strains due to the fibre and resin mismatch. Step 3 is summarised in Equation 5.

$$\boldsymbol{\varepsilon}^k = \mathbf{M}^k \left(\mathbf{E}^M + \mathbf{E}^T \right) + \mathbf{A}^k \Delta T \tag{5}$$

Dilatational and distortional strain invariants are evaluated at every sampling point, *k*, and compared to the corresponding critical strain invariants. Damage, defined as irreversible deformation, is predicted to occur when the inequality in Equation 6 is satisfied.

$$\max\left(\frac{\varepsilon_{dil}}{\varepsilon_{dil,crit}}, \frac{\varepsilon_{dis}}{\varepsilon_{dis,crit}} \right) \geq 1 \tag{6}$$

Damage onset within the fibre phase is not addressed in this paper.

2.4 Critical Invariants

The critical dilatational and distortional strain invariants are intrinsic material properties under Onset Theory. If the critical invariants are indeed intrinsic material properties, then the value for each invariant should be independently measurable using a number of lines of experiment/analysis. Two independent approaches are presented here: indirect measurement using unidirectional off-axis testing; and direct measurement using first principles thermodynamics (implemented in molecular dynamics simulation). Comparison of the two different approaches will be provided in a later section.

2.4.1 Critical Invariants derived from Unidirectional Testing

Currently the most practical way to determine the critical invariants for the matrix phase is indirectly via unidirectional off-axis tensile tests supported by complementary finite element analysis. The latest approaches reported in [9-11] propose a set of different off-axis unidirectional tests with off-axis angles from 10° to 90° to generate critical values of strain invariants for the matrix. Specimens with small off-axis angles, 0°-10°, will fail in the fibres and therefore are not included in the set for determining matrix failures. Unidirectional tests ensure that initiation of failure within the matrix phase immediately (or nearly immediately) results in failure of the entire specimen through the matrix, without fibre failure.

The axial failure strain for every test angle is recorded and then a simulation of the test is conducted using FE analysis. The specimen is then loaded until the global failure strain is reached. A critical value for both the dilatational and distortional strain invariants of the matrix can be found by evaluating the maximum dilatational and distortional invariants within the specimen domain (after dehomogenisation).

Robustness of this method is demonstrated by comparing tests of differing off-axis angles to ensure that, at specimen failure, the same strain invariant was present. Pipes and Gosse [12] and Ng et al [13] have demonstrated that shallow angle specimens, 10° to ~25°, give consistent critical invariants for distortional behaviour, while the remaining angles, ~25° to 90°, give consistent critical invariants for dilatational deformation. The cusp between the two failure mechanisms is not fixed, but depends on the relative magnitude of the two critical invariants.

2.4.2 Critical invariants from Molecular Dynamics

Independent of the experimental approach defined above, the critical invariants can be derived using atomistic simulation based on fundamental thermodynamic behaviour of polymers. It is a strong commendation of Onset Theory that two independent lines of evidence produce consistent critical material properties.

The procedure for determining the critical values of the dilatational and distortional invariants from an atomistic simulation were first published by Christensen [5]. It was found that the volumetric strain, ε_{dil}, which could be accommodated by an RVE of polymer material in MD simulation before irreversible deformation, was equal to the negative volumetric strain experienced during cooling from the glass transition temperature to the test temperature. Alternatively, if the distortion of the RVE, ε_{dis}, exceeded a critical value, then irreversible deformation would also occur.

Simulation results in Figure 2 were taken from Sul et al [6]. A simulation cell enclosing a model of the DGEBA/44DDS resin system with over 3000 atoms was subject to thermal and mechanical loads. The critical value for dilatation, $\varepsilon_{dil,crit}$, can be derived from Figure 2 and Equation 7.

$$\varepsilon_{dil,crit} = \frac{|\Delta V|}{V_0} = \frac{V_0 - V}{V_0} \tag{7}$$

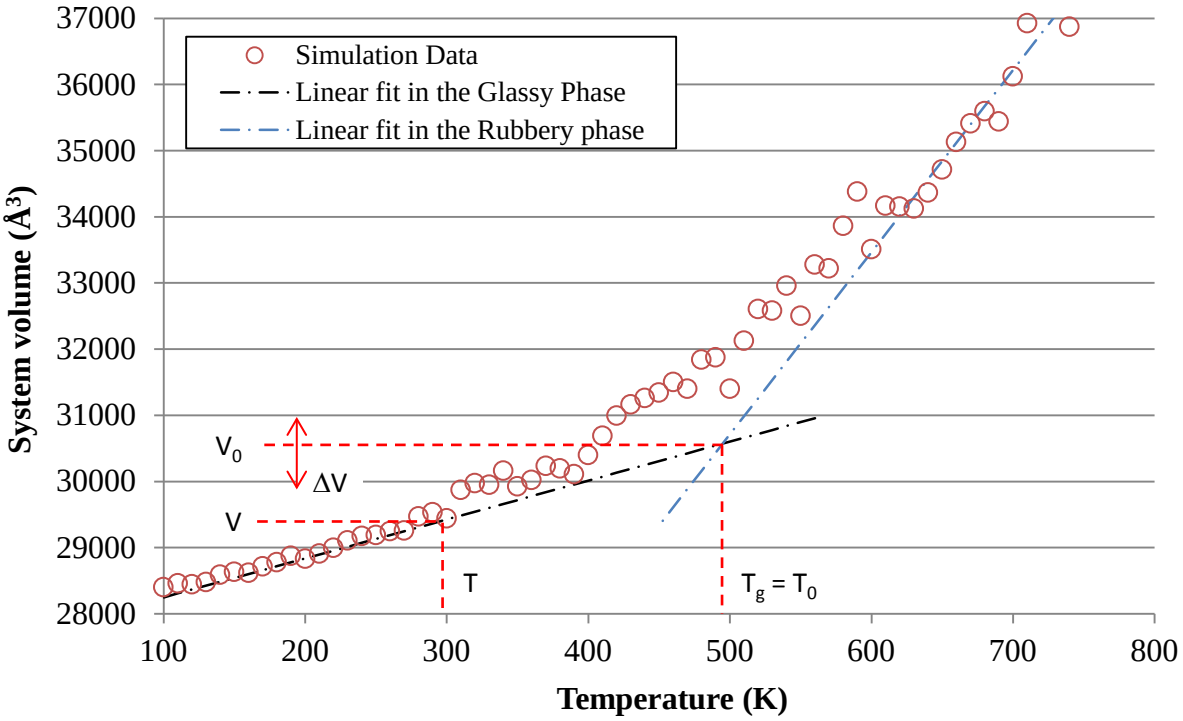

Figure 2: Volumetric change due to temperature cycle for volumetric strain for DGEBA / 44DDS [6]

A closed form estimate for $\varepsilon_{dil,crit}$ is available. The change in volume of the resin, δV, for a given small change in temperature, δT, can be determined from the CTE, α. Consider the volume change of a cube of isotropic resin with side length, L, subjected to a small positive temperature increment. The resulting volume change is shown in Figure 3.

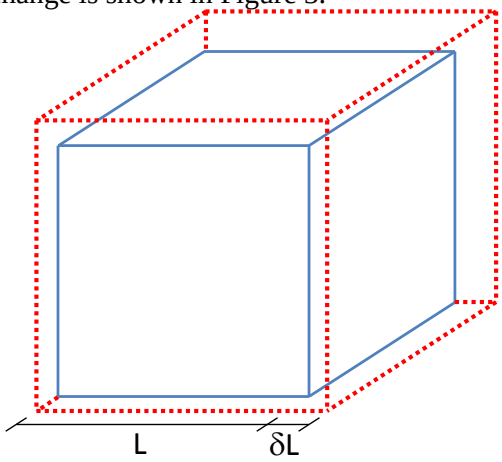

$$\delta V = (L+\delta L)^3 - L^3$$
$$\approx 3L^2\delta L$$
$$\delta L = \alpha L \delta T$$
$$\therefore \delta V \approx 3\alpha L^3 \delta T$$

Figure 3: Relationship between infinitesimal volume change and temperature change

If the CTE of the resin is constant over a finite temperature interval, ΔT, then the critical dilatational invariant can be found using Equation 8. Alternatively, if the CTE is a function of temperature, Equation 9 can be used.

$$\varepsilon_{dil,crit} = \frac{|\Delta V|}{V_0} = \frac{3\alpha L^3 |\Delta T|}{L^3} = 3\alpha |\Delta T| \quad (8)$$

$$\varepsilon_{dil,crit} = \frac{\left|\int_{V_0}^{V} \delta V\right|}{V_0} = \frac{3L^3\left|\int_{T_g}^{T} \alpha \delta T\right|}{L^3} = 3\left|\int_{T_g}^{T} \alpha \delta T\right| \tag{9}$$

It is apparent that the critical dilatational invariant is a function of temperature. This implies that homogenous, isotropic polymer matrices *increase* their capacity for dilatational deformation as temperature decreases, which may seem counter-intuitive. It should be noted however that thermal residual strains in the composite *also increase* as temperature decreases, offsetting, or in some cases overcoming, the increase in the critical material property.

The critical value of the distortional invariant, while not required for this paper, is obtained by plotting the stress calculated from the global pressure tensor in a simulation cell subject to strain at constant volume [5, 6, 14]. Non-linear behaviour in the stress-strain curve for a polymer before the peak stress is due to reversible dissipative processes occurring at the maximum level of torsional rearrangement. These processes are rate dependent and absorb mechanical energy, converting it to heat. The irreversible processes that define the distortional failure in Onset Theory do not appear until the reversible processes are exhausted. The critical distortional strain invariant can then be obtained from the stress-strain curve by measuring the applied strain at which the equivalent stress no longer increases as additional strain is applied (i.e. the slope of the curve is zero). When $\partial\sigma/\partial\varepsilon = 0$, the direct applied strain, ε_1, and the two components of transverse strain, ε_2 and ε_3, can be used with Equation 2 to find the critical dilatational strain invariant.

3 FABRIC ARCHITECTURES

3.1 Fabric modelling

A meso-mechanical RVE cell analysis for plain weave fabric architecture has been developed to dehomogenise continuum fabric lamina strains. The resin and tows of the RVE cell are modelled as continua, as shown in Figure 4, and the strains are initially resolved at this scale. A second application of dehomogenisation is required to resolve the strains in the resin between the individual fibres.

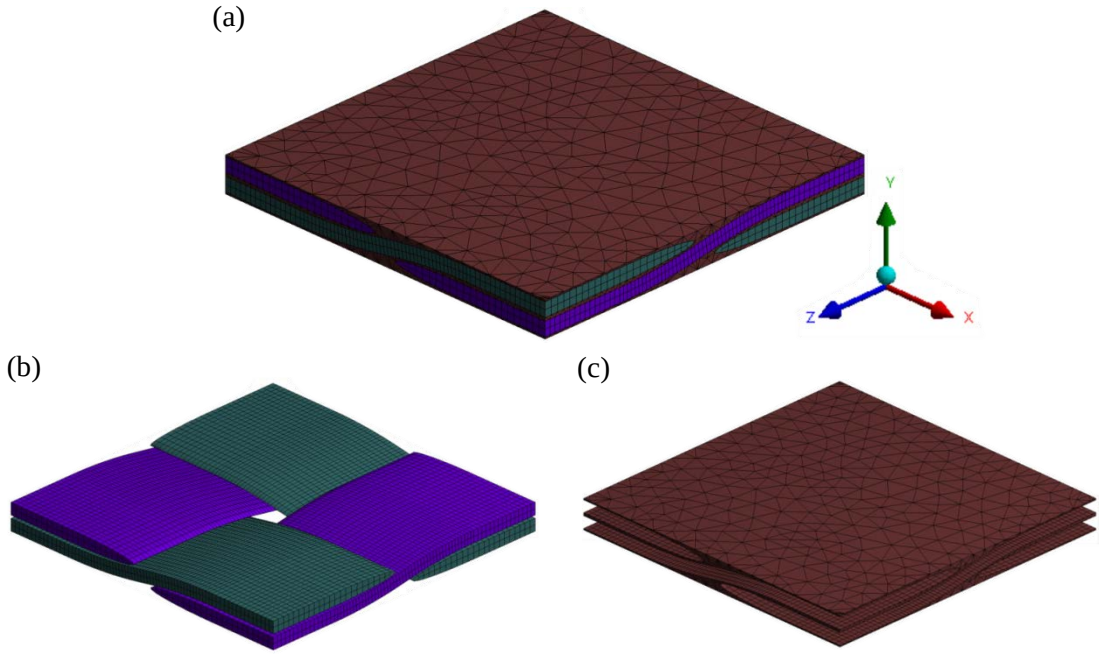

Figure 4: (a) RVE cell (b) tows and (c) resin part of the meso-mechanical unit cell model for strain dehomogenisation.

The material properties are applied parallel to the local axis of the tows to retain the accurate orthotropic behaviour during the cell analysis. The volume fraction of the tows to the unit cell is 80.84% which ensures an overall 60% fibre volume fraction. The dimensions of the unit cell are 2.56 x 2.56 x 0.25 mm to represent one layer thickness and one repeating unit of the in-plane fabric architecture. The tow major and minor axis ratio is set to be 18:1, where the minor axis is 0.1 mm. Extensional strain (boundary displacement) was applied to the surfaces perpendicular to x-axis. The other surfaces were constrained to remain planar with no net normal reaction force to represent symmetric free contraction boundaries.

A two-step analysis was applied for the fabric modelling (applied sequentially):

1. Thermal: Apply a ramped temperature from the cure temperature to the service temperature.
2. Mechanical: Apply a ramped mechanical strain from to zero to a large strain (equivalent to the axial failure strain) obtained from a tensile test of a $[0/90]_n$ fabric specimen.

At each step, the strain tensor at a range of critical locations within the tow domain was extracted and dehomogenised. From experience, the critical locations were within one of the transverse tows, highlighted by the yellow line in Figure 5.

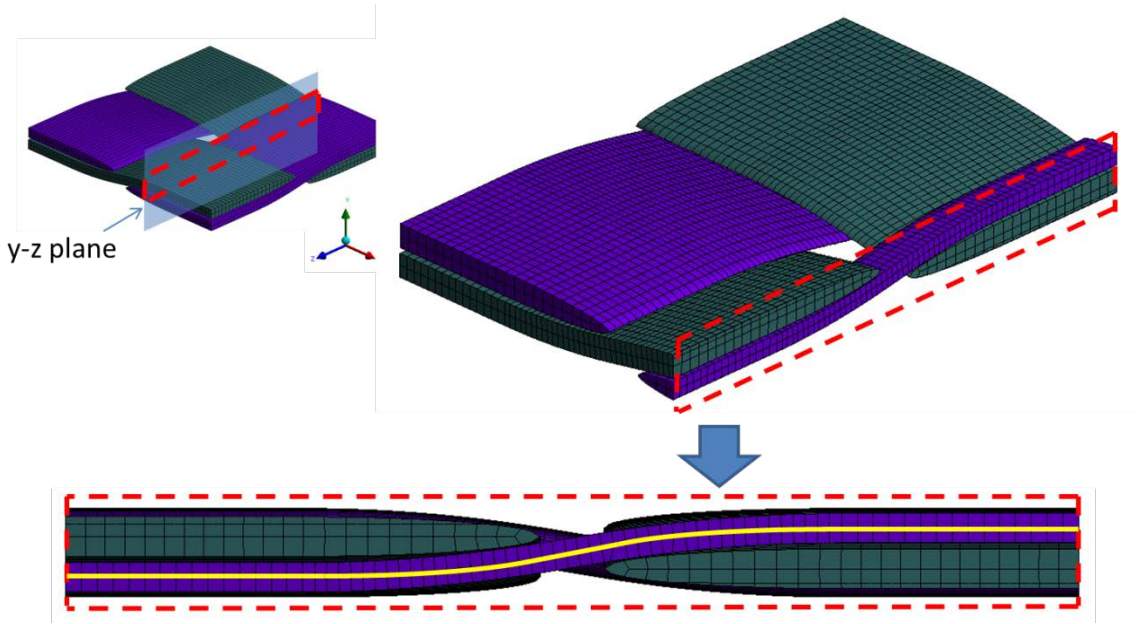

Figure 5: Path for extraction of strains in ANSYS (highlighted by the yellow line).

In this paper, the methodology is applied to two material systems – HTS40/RTM6 and T300/CYCOM970. The material properties to be applied to the tows and resin are given in Table 1.

Property	Unit	HTS40/RTM6 lamina	RTM6 Epoxy resin	T300/CYCOM970 lamina	CYCOM970 Epoxy resin
E_1	[GPa]	143.34	2.76	135	3.44
$E_2 = E_3$	[GPa]	8.34		8	
$G_{12} = G_{13}$	[GPa]	3.29	1	3.53	1.24
G_{23}	[GPa]	2.86		2.67	
$\nu_{12} = \nu_{13}$	-	0.25	0.38	0.27	0.39
ν_{23}	-	0.46		0.50	
α_{11}	[/°C]	$1.52X10^{-7}$	$57.6X10^{-6}$	$4.37X10^{-7}$	$80.6X10^{-6}$
$\alpha_{22} = \alpha_{33}$	[/°C]	$32.9X10^{-6}$		$46.2X10^{-6}$	
T_g	[°C]	-	185	-	170

Table 1: Properties of HTS40/RTM6 and T300/CYCOM970 material systems.

The critical dilatational invariant for the CYCOM970 resin system, derived experimentally, is 33500 με [4]. Based on the temperature dependent coefficient of thermal expansion of RTM6 resin [15], the critical dilatational invariant for RTM6 resin system, given by Equation 9, is 29624 με.

3.2 HTS40/RTM6

3.2.1 Experimental Investigation

Tensile tests were conducted on $[0/90]_{12}$ HTS40/RTM6 plain weave fabric specimens. The ultimate 'two-piece' failure strain was measured to be 1.2%. The specimen subjected to ultimate load was polished parallel to the specimen edge and examined for transverse microcracking. The resulting crack field is shown in Figure 6.

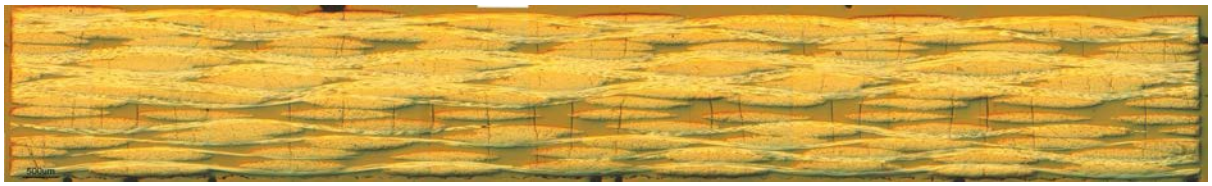

Figure 6: Surface microcracks for failed HTS40/RTM6 specimen.

In order to determine the strain at which the microcracking initiated, a number of specimens were loaded to varying strain levels up to the two-piece failure strain. Each specimen was polished and examined to confirm the existence of cracks. It was determined that the crack initiation strain was between 4800 and 6000 με.

3.2.2 Modelling

The influence of matrix plasticity and temperature dependent mechanical and thermal properties of the RTM6 resin [15] were applied in the two step fabric modelling analysis. Contour plots of dilatational and distortional invariants of the RVE cell model after step 2 are shown in Figure 7 and Figure 8 respectively.

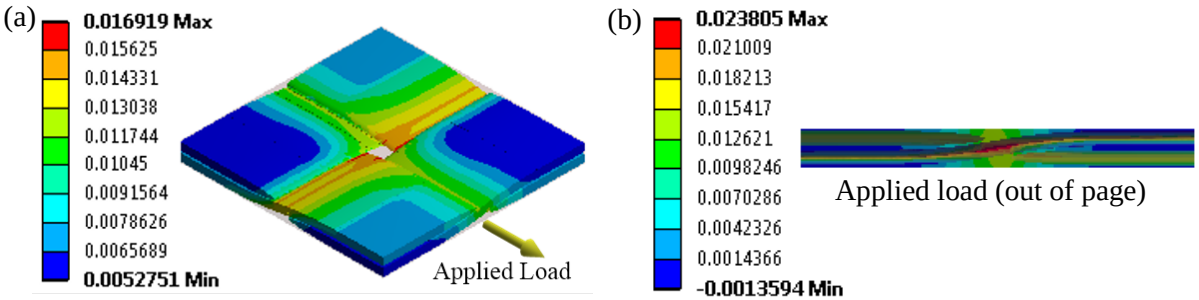

Figure 7: Dilatational invariant of the HTS40/RTM6 material system with (a) tows and (b) resin entities.

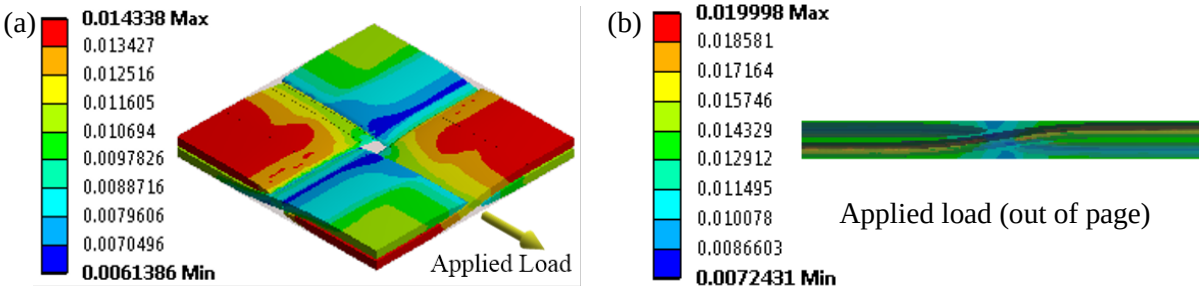

Figure 8: Distortional invariant of the HTS40/RTM6 material system with (a) tows and (b) resin entities.

The tows and resin have been separated for visualisation purposes. It should be noted that the strain in the tows has not yet been dehomogenised. The maximum dilatational and distortional invariants were located along the slender edge of the transverse tows. The maximum dilatational invariant was 23805 με and occurred directly adjacent to the large resin volume in the centre of the model. Meanwhile, the maximum distortional invariant was 19998 με and was located in the region where the tows overlapped one another.

The strain tensor was extracted along a path within the tow domain at the critical locations shown in Figure 5. The strain was subjected to a secondary dehomogenisation procedure (Equation 5) and the maximum invariants are summarised in Table 2. In this case failure is predicted to occur through dilatation within the transverse tow volume as the maximum dilatational strain invariant exceeds the critical dilatation invariant for RTM6, confirmed experimentally by Figure 6.

After Step	Maximum invariant	
	Dilatational (με)	Distortional (με)
1) Thermal	16100	29200
2) Mechanical	47900	53300

Table 2: Maximum invariants in the tows for HTS40/RTM6 material system.

The external mechanical strain was gradually increased from zero (in post-processing) to determine the strain at which transverse cracking onset initiated. Cracking was predicted when either (dehomogenised) strain invariant exceeded its critical value. The predicted axial mechanical strain when onset occurred was calculated to be 5107 με. Experimental observation indicated that the axial mechanical strain when onset occurred between 4800 to 6000 με and showed that the predicted value was in good agreement.

3.3 T300/CYCOM970

3.3.1 Experimental Investigation

Tensile tests were conducted on $[0/90]_{12}$ T300/CYCOM970 plain weave fabric specimens. The ultimate 'two-piece' failure strain was measured to be 1.3%. No matrix cracking was observed anywhere within the specimen domain except in the region of the ultimate fibre breakage location.

3.3.2 Modelling

The T300/CYCOM970 plain weave model results are shown in Figure 9 and Figure 10. As with the HTS40/RTM6 model, the results are shown at the ultimate failure strain and can be interpreted similarly. The maximum dilatational invariant in the neat resin was 26655 με and the maximum distortional invariant was 30344 με.

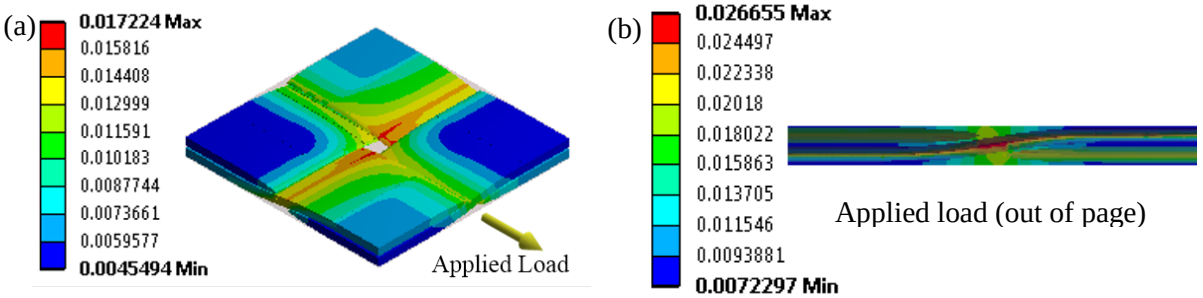

Figure 9: Dilatational invariant of the T300/CYCOM970 material system with (a) tows and (b) resin entities.

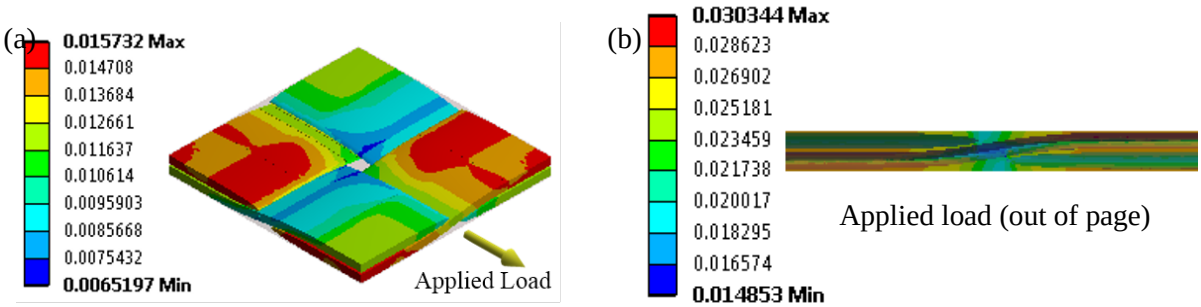

Figure 10: Distortional invariant of the T300/CYCOM970 material system with (a) tows and (b) resin entities.

The maximum invariants in the tows after the dehomogenisation procedure are shown in Table 3. Failure is predicted to occur through dilatation within the transverse tow volume as the maximum dilatational strain invariant exceeds the critical dilatation invariant for CYCOM970. The predicted axial mechanical strain when onset occurred is calculated to be 10833 με. Experimental observation indicated that no crack occurred prior to the failure strain. Although the theory and experimental results are not in perfect agreement, the theory did predict a far larger transverse cracking strain for the CYCOM970 system. Additional work is underway to experimentally determine the temperature dependent thermo-mechanical property set available for CYCOM970 resin. This may result in an increase in the crack onset predictions; bringing them more into line with experimental results.

After Step	Maximum invariant	
	Dilatational (με)	Distortional (με)
1) Thermal	17900	28600
2) Mechanical	37600	46300

Table 3: Maximum invariants in the tows for T300/CYCOM970 material system.

4 DISCUSSION AND CONCLUSIONS

Onset Theory for the prediction of the onset of failure in unidirectional composite laminates has been established by the work of Gosse. This paper extends the application of Onset Theory to the prediction of damage initiation sites in composite fabrics. The application to laminates manufactured from fabric plies required two levels of dehomogenisation. The first from the laminate to the fabric tow depends on the architecture of the fabric. The second level of dehomogenisation to the fibre/resin level requires the properties of the fibre and resin and includes the fibre volume fraction of the fibre within the fabric tow.

Onset Theory predicts the initiation of damage in the polymer resin at a molecular level. An additional increment of strain is required for the local polymer damage to grow into cracks that can be observed in the laminate. It is therefore anticipated that the failure prediction from Onset Theory will always underpredict the strain at which microcracking is observed. The more glassy the polymer matrix material, the closer the predictions should be.

It is clear from the results that predictions for RTM6 resin are well in line with observations whereas predictions for CYCOM970 slightly underpredict the strain to induce transverse cracking. Much of the disparity can be explained by considering the nature of the resin. RTM6 is a glassy system to which no toughening agents have been added. CYCOM970 includes a precipitation toughener which is expected to influence the initial growth of the microcracks. Further work is required to observe the true onset of irreversible deformation in toughened epoxy systems; further work is also required to theoretically account for the extent to which resin toughening affects the transition of polymer damage to microscopically observable damage.

ACKNOWLEDGEMENTS

This project has been supported by the Australian Research Council Linkage Grant LP100200607. Dr Jon Gosse, Mr Steve Christensen and Mr Steve Georgiadis from The Boeing Company are gratefully acknowledged for specimen preparation, critical insight and technical input.

REFERENCES

1. Gosse, J.H. and S. Christensen, *Strain Invariant Failure Criteria for Polymers in Composite Materials*, in *42nd AIAA Structures, Structural Dynamics and Materials Conference and Exhibit*. 2001: Seattle.
2. Pipes, R.B. and J.H. Gosse, *An onset theory for irreversible deformation in composite materials.* ICCM-17, the 17th International Conference on Composite Materials, Edinburgh, UK, 27-31 Jul 2009, 2009.
3. Tran, T., et al., *A micromechanical sub-modelling technique for implementing Onset Theory*. Composite Structures, 2013. **103**: p. 1-8.
4. Tran, T.D., et al., *Micromechanical modelling for onset of distortional matrix damage of fiber reinforced composite materials.* Composite Structures, 2012. **94**(2): p. 745-757.
5. Christensen, S., *Using Molecular Dynamics Coupled with Higher Lengthscale Simulations for the Development of Improved Composite Matrix Materials*, in *17th International Conference on Composite Materials*. 2009: Edinburgh.
6. Sul, J.-H., B.G. Prusty, and D.W. Kelly, *Application of molecular dynamics to evaluate the design performance of low aspect ratio carbon nanotubes in fibre reinforced polymer resin.* Composites Part A: Applied Science and Manufacturing, 2014. **65**: p. 64-72.
7. Sul, J.-H., B. Gangadhara Prusty, and D.W. Kelly, *Molecular dynamics study on effects of aspect ratio of carbon nanotubes in thermosetting epoxy based nanocomposites including modeling of crosslinking process.* Advanced Manufacturing: Polymer & Composites Science, 2015. **1**(2): p. 94-104.
8. Sul, J., et al., *Failure study for thermosetting epoxy in composite materials using onset theory in conjunction with molecular dynamics*, in *ICCS17 - 17th International Conference on Composite Structures*, A.J.M. Ferreira, Editor. 2013: Porto, Portugal.
9. Buchanan, D.L., et al., *Micromechanical enhancement of the macroscopic strain state for advanced composite materials.* Composites Science and Technology, 2009. **69**(11-12): p. 1974-1978.
10. Pearce, G.M., et al., *Atoms to assemblies: A physics-based hierarchical modelling approach for polymer composite components.* Applied Mechanics and Materials, 2014. **553**: p. 41-47.
11. Tran, T., *Development of micromechanical modelling procedures using the onset theory for failure of composites*, in *School of Mechanical and Manufacturing Engineering*. 2012, University of New South Wales: Sydney, Australia.
12. Byron Pipes, R., et al., *Interlaminar stresses in composite laminates: Thermoelastic deformation.* Composites Science and Technology, 2010. **70**(11): p. 1605-1611.
13. Ng, S.J., et al., *SIFT analysis of IM7/5250-4 composites*, in *36th International SAMPE Technical Conference - Materials and Processing*. 2004, Society for Advancement of Material and Processing Engineering: San Diego. p. 129-141.
14. Christensen, S. and R. D'Oyen, *Computational formulation of a new composite matrix.* Scripta Materialia, 2014. **70**: p. 18-24.
15. Hobbiebrunken, T., et al., *Microscopic yielding of CF/epoxy composites and the effect on the formation of thermal residual stresses.* Composites Science and Technology, 2005. **65**(10): p. 1626-1635.